

Synthesis of graphene-oxadiazole-2-thiol (RGS) / PVA composite and studying Its electric properties

Ibrahim F. waheed¹, Emaad T. Bakir¹, Sabah M. Ali²

¹ Department of chemistry , College of Science, Tikrit University, Tikrit , Iraq.

² Department of Physics , College of Education For Pure Science, Kirkuk University , Kirkuk , Iraq.

imaofs83@yahoo.com , emaad_bakir@yahoo.com , sabah_vagmur@yahoo.com

Abstract

In this work focused on preparing novel nanocompound Reduce graphene-oxadiazole-2-thiol (RGS), is a derivative of graphene, Which was obtained through a series of reactions on graphene oxide (GO). Incorporating (RGS) in PVA via non-covalent afforded RGS/PVA composites with different weight of RGS. the RGS/PVA composite and pure PVA were identified by different techniques, FTIR measurements, The scanning electron microscope (SEM), powder x-ray diffraction. The electrical properties of the RGS/PVA composite was investigated. These properties include dielectric constant, permittivity(ϵ'), imaginary permittivity(ϵ''), conductivity (σ_{AC}) and loss factor ($\tan \delta$). The measurements were performed at frequencies (5000Hz-1MHz) at room temperature.

Key words: graphene-oxadiazole-2-thiol (RGS), x-ray diffraction, dielectric constant.

1. Introduction

Graphene is a flat monolayer of carbon atoms. with a carbon-carbon distance of 0.142 nm is the first truly two-dimensional (2D) crystalline material, without any doubt, which is stable at room conditions and which is bonded together in a hexagonal lattice, completely conjugated sp^2 hybridized planar structure and is a basic building block for graphitic materials of all other dimensionalities. It can be wrapped up into 0D fullerenes, rolled into 1D nanotube or stacked into 3D graphite [1-6]. The synthesis is correlated to the outstanding properties of graphene. For instance, due to its unique edge atomic configuration and electronic band structures, graphene exhibits novel transport effects, such as the ambipolar field effect and minimum conductivity that lead to exceptional transport properties such as quantum Hall effects, and a high mobility of carriers [7]. It was reported that by modifying the structure of graphene (basal planes or edges) it is possible to tailor the graphene properties and produce new types of graphene-based materials, which can be employed for the design of nanoscale transistors [8], gas sensors [9], fuel cells [10], solar cells[11], organic light-emitting diodes (OLEDs) displays [12,13], and bio-related sensors [14]. porous graphene (PG), a graphene based material, is attracting the interest of many researchers[15]. The present work focuses on the preparation one of the derivatives of graphene sheets is grapheme - oxadiazole-2-thiol (RGS). Incorporating (RGS) in PVA via non-covalent afforded RGS / PVA composites with different weight of RGS and study of properties thermal and electrical for Fabrication films by TGA and LCR meter.

2. Experimental section

2.1 Materials

The starting materials used were obtained from different sources and companies like Sodium nitrate (Merck co.), Graphite (Appelchem co.), Potassium Permanganate, Sulphuric acid, Potassium hydroxide and Carbon disulfide (Sigma-Aldrich co.), Hydrogen peroxide (HIMIDIA co.), Hydrazine mono hydrate

(Qualikems co.), Poly (vinylalcohol) (PVA) (AFCO co.)

2.2 Preparation of Graphene -oxadiazole-2-thiol (RGS).

GO was prepared following a modified Hummers method from graphite powders (after oxidation of graphite by Hummers method the functional groups for GO: epoxide, hydroxyl, carboxylic)[16]. Dried GO powder was dispersed into water to create a dispersion of 100 mg/mL. Exfoliation of GO to graphene oxide was achieved by ultrasonication of the dispersion for 1 h. Hydrazine hydrate (1.00 ml, 32.1 mmol) was then added and the solution heated in an oil bath at 100°C under a water-cooled condenser for 24h reflux. The reduced graphene oxide (RGO) gradually precipitated out as a black powder. Dried RGO powder was dispersed into methanol (75ml) to create a dispersion of 1000 mg/ ml, Carefully add (5 ml) conc. sulfuric acid, then reflux the solution for 13 h. After refluxing, the resulting suspension was filtered, washed with distilled water, and dried under vacuum for 24 h. to obtain Ester- Graphene (RGE). The dry RGE powder was dispersed into hydrazine hydrate (50ml) to create a dispersion of 500 mg/ ml. yielding an in homogeneous black dispersion solution. then reflux the solution for 30 h. the resulting suspension was filtered, washed with distilled water, and dried under vacuum for 24 h. to obtain Graphene hydrazide (RGH). potassium hydroxide (0.5g) was loaded in a 250 ml round bottomed flask and ethanol (75ml) was then added, then RGH (0.2g) added. After that a solution of stirring for 2 h. at room temperature, the mixture round bottomed flask put into ice path and carbon disulfide (0.1ml) was in small portions with constant stirring noted change in color to black greenish, then reflux the solution for 24 h. Finally, the resulting suspension was filtered, wash with the amount of HCl diluted, and dried under vacuum for 24 h. to obtain Graphene -oxadiazole-2-thiol (RGS).

2.3 Fabrication of RGS/PVA composites

Polymeric nano Composites films of different weight percent concentrations are prepared. These films contain different proportions of RGS was added to the PVA solutions (25ml). Then, mixture exposed to sonication for (10-15) min to ensure dispersion of the nanosheets between the polymer chains, after the sonication, and mixed by magnetic stirrer for few seconds. Then, the mixture was poured into the specific glass mold and left overnight. Then, the film was peeled out and dried under vacuum for 4 h., to obtain dry films.

2.4. Characterization

Fourier transform infrared spectroscopy (FT-IR) measurements were carried out by using a shimadzu 8400 spectrophotometer over the range of (4000-400) cm^{-1} . Scanning electron microscope (SEM) observation was performed on a Hitachi S-4700 microscope with an accelerating voltage of 20 kV. Transmission electron microscope. X-ray diffraction (XRD) analysis was carried out with a Rigaka D/max 2500 diffractometer using a Cu Ka radiation source. Dielectric properties of the RGS/PVA composites were measured by using LCR meter type PM6036, were studied by measurement of real, imaginary permittivity, loss factor ($\tan \delta$) and the Ac conductivity (σ_{Ac}). The investigations were made at different frequencies (5000Hz-1MHz) at room temperature. The dielectric parameter as a function of frequency is described by the complex permittivity

$$\varepsilon^*(\omega) = \varepsilon'(\omega) - j\varepsilon''(\omega) \dots (1)$$

where the real part ε' and imaginary part ε'' are the components for the energy storage and energy loss,

respectively, in each cycle of the electric field. (ω) is the angular frequency; $\omega = 2\pi f$, f is applied frequency. The measured capacitance, C was used to calculate the dielectric constant, ε' using the following expression.

$$\varepsilon' = Cd / \varepsilon_0 A \dots (2)$$

where d is the thickness between the two electrodes (film thickness), A is the area of the electrodes, ε_0 is permittivity of the free space, $\varepsilon_0 = 8.85 \times 10^{-12} \text{ F.m}^{-1}$ and whereas for dielectric loss $\varepsilon''(\omega)$, and $\tan \delta$ is tangent delta[17]:

$$\varepsilon''(\omega) = \varepsilon'(\omega) \cdot \tan \delta(\omega) \dots (3)$$

The AC conductivity (σ_{ac}) can be calculated by the following equation[17]:

$$\sigma = \varepsilon_0 \varepsilon' \omega \tan \delta \dots (4)$$

3. Results and discussion

In Fig.1 FTIR spectrum of RGS is showed. It clearly reveals the major peaks associated with RGS, such as band weak at (3440) cm^{-1} denoting $\nu(\text{N-H})$ stretching vibration of secondary amine, absorption band weak in the region (2385) cm^{-1} denoting $\nu(\text{S-H})$, absorption peak at the region (1652) cm^{-1} denoting $\nu(\text{C=N oxadiazole})$, absorption peak at the region (1558) cm^{-1} denoting $\nu(\text{C=C})$. In addition, peaks at (1458) cm^{-1} and at (1027) cm^{-1} appeared, which correspond to $\nu(\text{C-N})$ and $\nu(\text{C-O oxadiazole})$ stretching vibration, respectively[18]. which suggests that the reaction cyclization had been successfully on the surface of the RGS sheets. FT-IR spectra for nanosheets (GO, RGO, RGH, RGE and RGS) were collected and are presented in Fig. 1.

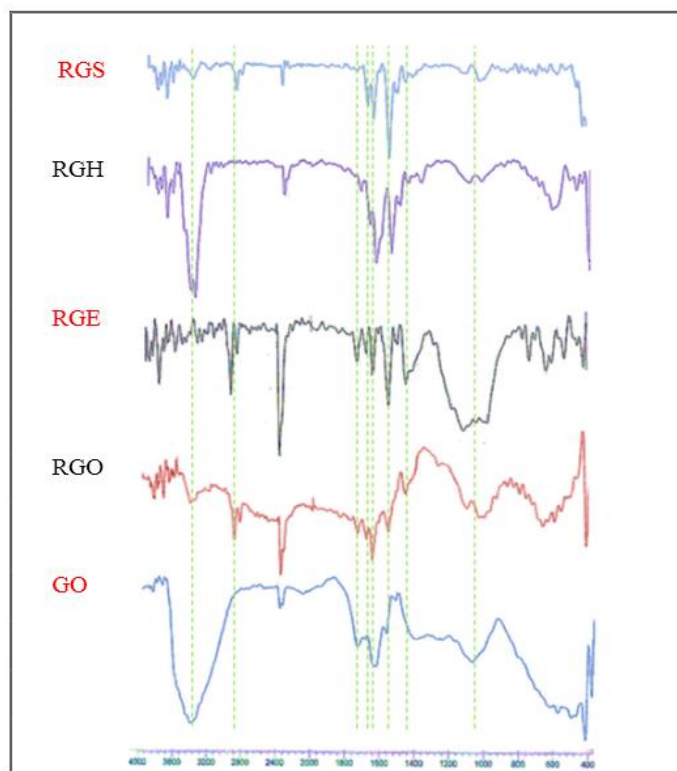


Fig.1 FTIR spectra of GO, RGO, RGE, RGH and RGS

From Fig.2 noted that XRD pattern of GO indicates a larger interlayer spacing in GO than in RGO. Water molecules, as well as the formation of oxygen-containing groups between the layers during the preparation of GO result in a lower angle reflection peak $2\theta = 11.86$ (d-spacing 7.71 \AA). The decrease in the interlayer spacing in RGO and the shift of the low peak at higher 2θ angles (26.19 , d-spacing 3.4 \AA) verify the efficient reduction by hydrazine method,

due to the more through removal of surface functional group. In the case of RGO, RGE, RGH and RGS respectively, we note that there is increasing in intensity this can be ascribed to the an increase in atomic weight therefore in the case of RGO reflection at $2\theta = 26.19^\circ$ becomes wider, the crystallinity of the RGO sample deteriorates, which indicates a decrease in the size of particles[19,20].

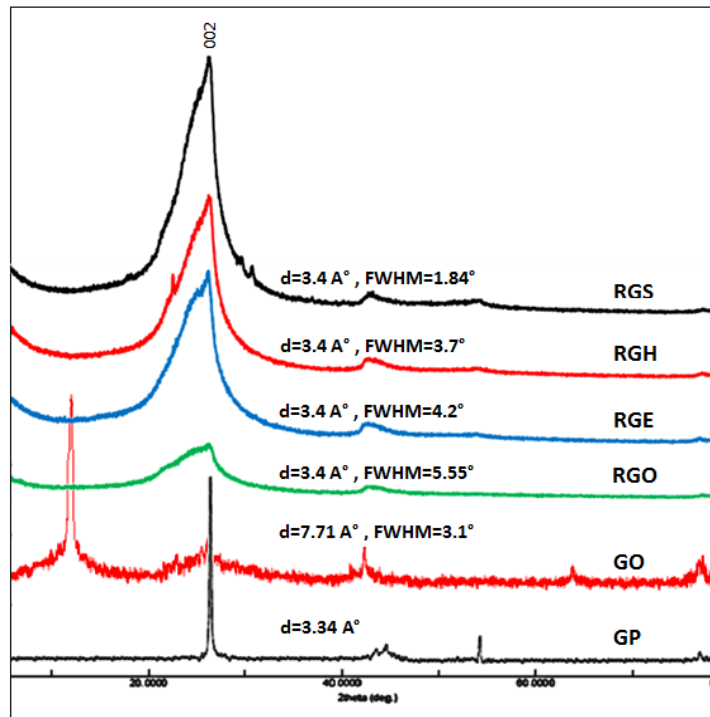


Fig.2 X-Ray Diffraction patterns of GP , GO , RGO , RGE, RGH and RGS

Based on X-ray diffraction characterization has been done resulting some of the main peak at 2θ position of 19.4° , 26.19° and 43.2° with each field orientation is (110) (002) and (100), while the peak of the diffraction pattern PVA as the matrix contained in the plane orientation (110) with the angular position 19.4° . Fig.3. However, after RGS is dispersed into the

PVA matrix, the XRD pattern of the RGS/PVA nanocomposites show the PVA peak and significant decrease in the intensity of RGS diffraction peaks. This result demonstrates that RGS is fully exfoliated into single RGS sheets in the PVA matrix[21,22]. This is consistent with SEM, which we got was.

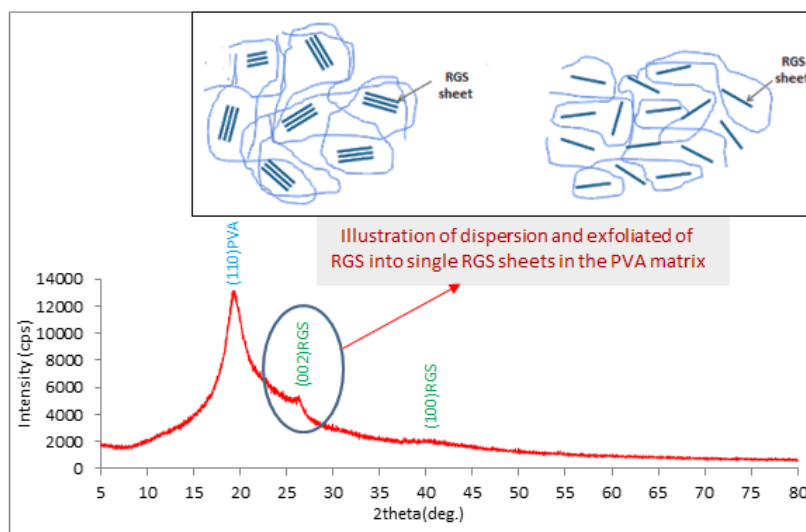


Fig.3 X-Ray Diffraction patterns of RGS/PVA nanocomposite

A scanning electron microscope (SEM) is a type of electron microscope that images a sample by scanning it with a high-energy beam of electrons in a raster scan pattern. The electrons interact with the atoms that make up the sample producing signals that contain information about the sample's surface topography, composition, and other properties such as electrical conductivity. Fig.4a shows scanning electron microscope images (SEM) of RGS, which was obtained after several chemical reactions. The RGS sheets formed showed wrinkled appearance and appear to be very thin and is apparently that there are

many crumpling on the surface of RGS which come from the scrolling of RGS sheets. The wrinkled nanostructure of RGS sheets could provide a larger active area for the deposition of heavy metal ions. Fig.4b shows SEM cross-section micrographs of the RGS/PVA after drying. The SEM images clearly indicate that the RGS are well-dispersed and partially aligned in the PVA matrix, the RGS nanosheets are arranged as a 3D network throughout the PVA polymer matrix, and hydrogen bonding formed between PVA and RGS. According to a report by Zhao et al.[23].

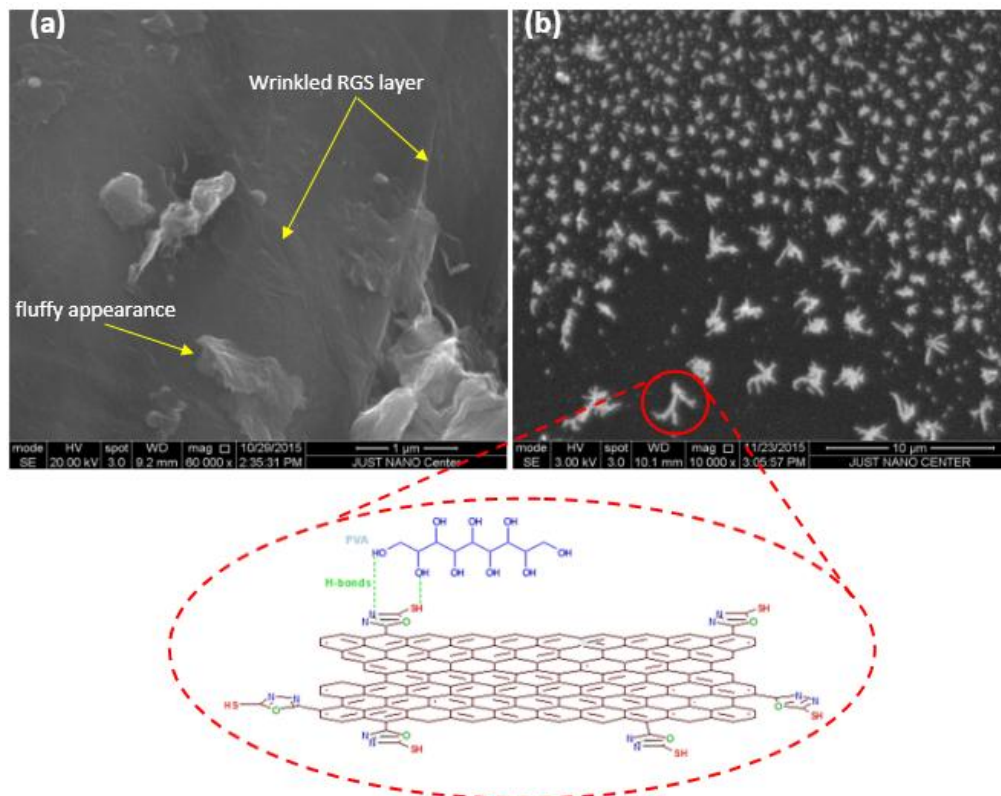


Fig.4 The SEM images of (a) RGS and (b) RGS /PVA matrix

3.1 Electrical Properties

Fig.5a-d shows the dielectric permittivity (ϵ'), imaginary permittivity (ϵ''), conductivity (σ_{Ac}) and loss factor ($\tan \delta$) of the (1w%, 4w% and 8w%) RGS/PVA composites as a function of frequency at room temperature. The dielectric permittivity ϵ' , which is also known as the relative dielectric constant, is the real part of the complex dielectric permittivity. The loss factor ($\tan \delta = \epsilon''/\epsilon'$) is commonly used as a measure of the energy dissipation in a dielectric material. As expected, dielectric properties of the RGS/PVA composites show a typical percolation transition behavior as the concentration of RGS incorporated within the PVA matrix increases. In the studied frequency range of (10^3 - 10^6) Hz, the dielectric permittivity of dried PVA latex gradually decreases from 4.34 to 3.53 as the frequency increases. It can be clearly observed that

the dielectric permittivity of the composites can be enhanced by blending with RGS nanosheets. At low RGS concentration, the dielectric permittivity of the RGS/PVA composites still exhibits a slow decrease trend along with the increasing frequency. For example, the dielectric permittivity of the composite (1wt%) shows a gradual decrease from 4.84 to 4.56. When the RGS content approached about (4wt%), a percolation transition from an insulator to conductor occurred, which is accompanied by a dramatically increased dielectric permittivity. The dielectric loss of the RGS/PVA composites is also substantially improved due to the incorporation of conductive RGS nanosheets. For the composite with the RGS content of (4wt%), its loss factor is about a magnitude higher than that of dried PVA latex in the lower frequency region. The loss factor of the composite (8wt%) at 10^4 Hz goes up to an even higher value. Such increase

in the loss factor is the inevitable consequence of the significantly enhanced conductivity of the RGS/PVA composites and could be considered as one important feature of the percolative composites. For composites incorporated with conductive fillers, the dielectric loss is mainly caused by the leakage current in the composites. Higher content of conductive fillers could construct more conductive pathways, and thus result in more significant leakage current and dielectric loss. Fig.5d displays the frequency dependence of AC conductivity (σ) of the RGS/PVA

composites with different RGS contents. For the composites with low RGS contents (4 wt%), the conductivity curves show a strong dependence on frequency owing to their insulating nature. The AC conductivity of the composites increases with the increasing frequency. An insulator-semiconductor transition is clearly observed when the RGS loading exceeds (4wt%). These results are in good agreement with the variation of dielectric properties of the RGS/PVA composites[24].

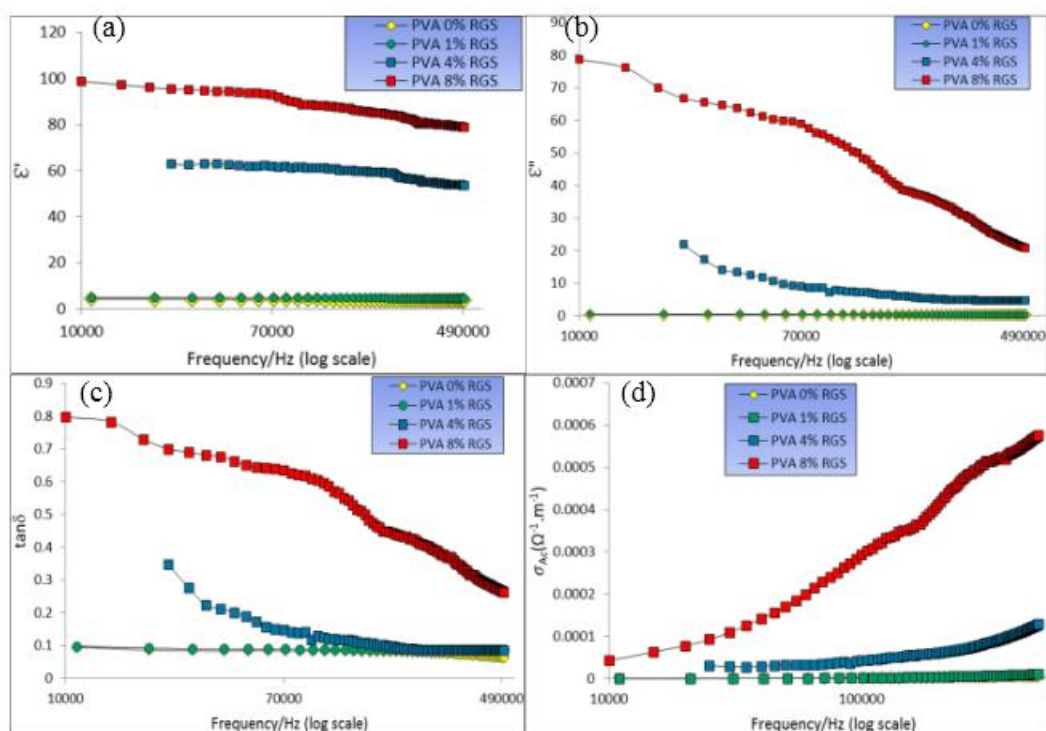


Fig.5 (a) Dielectric permittivity (ϵ') (b) imaginary permittivity (ϵ'') (c) loss factor ($\tan \delta$) and (d) conductivity (σ) of the RGS/PVA composites with different concentration of NFNPs as a function of frequency at room temperature.

Conclusions

We have successfully synthesized high-performance RGS/PVA, nanocomposites by incorporating RGS into PVA aqueous solution. From the previous discussed results we can imply that the interplanar spacing of the RGS with PVA is broadened due to possible intercalation of PVA leading to fully

References

- [1] J. Lahiri, Y. Lin, P. Bozkurt, I.I. Oleynik, M. Batzill, *Nature Nanotechnology*, 5 (2010) 326-329.
- [2] M. Terrones, O. Martin, M. Gonzalez, J. Pozuelo, B. Serrano, J.C. Cabanelas, S.M. Vega-Diaz, *Advanced Materials*, 10 (2011) 5302.
- [3] H.O. Pierson, *Handbook of carbon, graphite, diamond and fullerenes*. NJ, USA: Noyes; (1993).
- [4] L. Dai, D.W. Chang, J.B. Baek, W. Lu, *Small*, 8 (2012) 1130-1166.
- [5] D.R. Dreyer, R.S. Ruoff, C.W. Bielawski, *Angew Chem Int Ed*, 51 (2012) 7640-7654.

exfoliated RGS by treatment with PVA. The synthesized composites exhibited a significant improvement in electrical properties at a low loading of RGS compared to pure PVA. Moreover, RGS is an effective nanofiller, and can be used for many practical nanocomposites.

- [6] K.S. Novoselov, V.I. Falco, L. Colombo, P.R. Gellert, M.G. Schwab, K. Kim, *Nature*, 490 (2012) 192-200.
- [7] W. Choi, J-W. Lee, "Graphene: Synthesis and Applications", CRC Press, Taylor & Francis group, (2012).
- [8] X. Wang, X. Li, L. Zhang, Y. Yoon, P. K. Weber, H. Wang, J. Guo, H. Dai, *Science* 324(5928) (2009) 768-771.
- [9] K.S. Novoselov, A.K. Geim, S.V. Morozov, D. Jiang, Y. Zhang, S.V. Dubonos, I.V. Grigorieva, A.A. Firsov, *Science*, 306 (2004) 666-669.

- [10] Y. Shao, S. Zhang, M. H. Engelhard, G. Li, G. Shao, Y. Wang, J. Liu, I. A. Aksay, Y. Lin, *J. Mater. Chem.* 20 (2010) 7491-7496.
- [11] X. Wang, L. Zhi, K. M'ullen, *Nano Lett.* 8(1) (2008) 323-327.
- [12] D. Kim, D. Lee, Y. Lee, *Adv. Funct. Mater.* 23(40), (2013) 5049-5055.
- [13] J. Ha, S. Park, D. Kim, J. Ryu, C. Lee, B. H. Hong, Y. Hong, *Organic Electronics* 14(9) (2013) 2324-2330.
- [14] X. Michalet, F. F. Pinaud, L. A. Bentolila, J. M. Tsay, S. Doose, J. J. Li, G. Sundaresan, A. M. Wu, S. S. Gambhir, *Science* 307(5709) (2005) 538-544.
- [15] B. D. Zdravkov, J. J. Cermak, M. Sefara, J. Jank, *Cent. Eur. J. Chem.*, 5(2), (2007) 385-395.
- [16] W.S. Hummers Jr., R.E. Offeman, *Journal of the American Chemical Society* 80 (6) (1958) 1339-1339.
- [17] S. Stankovich, D.A. Dikin, R.D. Piner, K.A. Kohlhaas, A. Kleinhammes, Y. Jia, Y. Wu, S.T. Nguyen, R.S. Ruoff, *Carbon*, 45 (2007) 1558-1565.
- [18] C.W.M. Yuen, S.K.A. Ku, P.S.R. Choi, C.W. Kan, *RJTA*, 9(2)(2005)26-38.
- [19] P. Sungjin, A. Jinho, J.R. Potts, A. Velamakanni, S. Murali, R.S. Ruoff, *Carbon*, 49 (2011) 3019-3023.
- [20] M.O. Danilov, I.A. Slobodyanyuk, I.A. Rusetskii1, G.I. Dovbeshko, *Nanoscience and Nanotechnology Research*, (2) (1) (2014) 12-17.
- [21] B.W. Chieng, N.A. Ibrahim, W. M. Z. W. Yunus, M.Z. Hussein, Y.Y. Then, Y.Y. Loo, *Polymers*, 6 (2014) 2232-2246.
- [22] J. Wang, X. Wang, C. Xu, M. Zhanga, *Polym Int*, 60 (2011) 816-822.
- [23] X. Zhao, Q. Zhang, D. Chen, *Macromolecules.*, 43(2010) 2357-2363.
- [24] D. Wang, X. Zhang, J. Zha, J. Zhao, Z. Dang, G. Hub, *Polymer* 54 (2013) 1916-1922.

تحضير المركب كرافين-أوكسادايازول-2-ثايول (RGS/PVA) ودراسة خصائصه الكهربائية

ابراهيم فهد وحيد¹, عماد طه بكر¹, صباح محمد علي²

¹قسم الكيمياء، كلية العلوم، جامعة تكريت، تكريت، العراق

²قسم الفيزياء، كلية التربية للعلوم الصرفة، جامعة كركوك، كركوك، العراق

emaad_bakir@yahoo.com, imaofs83@yahoo.com, yagmur@yahoo.com

الملخص

في هذا البحث ركزنا على تحضير مركب عضوي نانوي جديد وهو Reduce graphene-oxadiazole-2-thiol (RGS) حيث يتم تحضير هذا المركب من خلال سلسلة تفاعلات تجرى على اوكسيد الكرافين (GO). دمج (RGS) مع البولي فنيل الكحول (PVA) عن طريق الارتباط غير التساهمي حيث نحصل على التركيب RGS/PVA وينسب مختلفة من (RGS). شخص كل من PVA النقي والمركب RGS/PVA بتقنيات مختلفة بواسطة الاشعة تحت الحمراء (FTIR) والمجهر الالكتروني (SEM) وحيود الاشعة السينية للمسحوق (RXD). درست الصفات الكهربائية للمركب RGS/PVA حيث شملت السماحية الحقيقية (ϵ') والخيالية (ϵ''), والتوصيلية الكهربائية (σ_{AC}) وعامل الخسارة ($\tan \delta$). حيث اجريت هذه القياسات في الترددات (5000Hz-1MHz) وفي درجة حرارة الغرفة.

الكلمات المفتاحية: كرافين-أوكسادايازول-2-ثايول (RGS), حيود الأشعة السينية (XRD), ثابت العزل الكهربائي.